The effect of temperature and fuel surface area on spent nuclear fuel dissolution kinetics under H2 atmosphere

Journal of Nuclear Materials 531 (2020) 151981

Contents lists available at ScienceDirect

Journal of Nuclear Materials

journal homepage: www.elsevier.com/locate/jnucmat

The effect of temperature and fuel surface area on spent nuclear fuel dissolution kinetics under H_2 atmosphere

Ella Ekeroth [a, c], Michael Granfors [a], Dieter Schild [b], Kastriot Spahiu [c, d, *]

[a] Studsvik Nuclear AB, SE - 611 82, Nyköping, Sweden
[b] KIT-INE, P.O. Box 3640, 76021, Karlsruhe, Germany
[c] SKB, Box 3091, SE - 169 03, Solna, Sweden
[d] CTH, Kemivägen 4, SE-43267, Gothenburg, Sweden

ARTICLE INFO

Article history:
Received 7 October 2019
Received in revised form
15 December 2019
Accepted 29 December 2019
Available online 1 January 2020

ABSTRACT

In this work we present the results of two spent nuclear fuel leaching experiments in simulated granitic groundwater, saturated with hydrogen under various pressures. The results show a large impact of the dissolved hydrogen already at 1 bar H_2 and room temperature on the release of both the uranium and of the fission products contained in the fuel matrix. Based on the results of this study and on published data with fuel from the same rod, the importance of the oxidative dissolution of spent fuel under repository conditions as compared to its non-oxidative dissolution is discussed. The XPS-spectra of the fuel surface before the tests and after long-term leaching under hydrogen are reported and compared to reduced UO_2 and SIMFUEL surfaces. The overall conclusion is that in spite of the unavoidable air contamination, hydrogen pressures of 1 bar or higher counteract successfully the oxidative dissolution of the spent nuclear fuel. The stability of the 4d-element metallic particles during fuel leaching under such conditions is also discussed, based on data for their dissolution. The metallic particles are also stable under such conditions and are not expected to release their component metals during long-term fuel leaching.

1. Introduction

The direct disposal of spent nuclear fuel as a waste form is currently under consideration in several countries. In most disposal concepts for high-level waste, spent nuclear fuel will be encapsulated in massive canisters made of or containing large amounts of metallic iron. The canisters will then be placed in deep underground repositories built at several hundred meters depth in granitic, clay or salt bedrocks. In most concepts, each canister will be surrounded by compacted bentonite clay. This arrangement constitutes a multiple barrier system, including the engineered or technical barrier (waste form and backfill materials) and the geologic barrier (the host rock formation itself and its overburden). All barriers contribute to isolate the radionuclides from the biosphere by retardation of groundwater access and by their retention on solid surfaces present in the repository. Additionally, an engineered barrier may affect the geochemical environment to provide favourable conditions with respect to low solubilities of radionuclides and low dissolution rates of waste forms.

The chemical form of uranium in light-water reactors (LWR) fuel is nearly stoichiometric uranium dioxide, both before and after irradiation, with only a small fraction of other actinides and fission products. The higher actinides produced by capture of epithermal neutrons are generally considered to form solid solutions with UO_2(s) [1]. The chemical state of the fission products and the microstructure of nuclear fuel have been studied extensively [1–4] and only a short summary is given below. Fission products which are stable in metallic form (Mo, Ru, Pd, Tc, Rh) tend to form metallic alloy particles, often referred to as 4d-alloy particles or ε-particles. Fission products which are stable as oxides, but incompatible with the UO_2 matrix (Rb, Cs, Ba, Zr, Nb, Mo, Te, Sr) separate into precipitates sometimes referred to as grey phases. The general composition of these grey phases is ABO_3, with Ba, Sr, and Cs in the A sites and Zr, Mo, U, Pu, and lanthanides in the B sites, crystallizing in a cubic perovskite–type structure. Elements that form stable oxides in solid solution with UO_2 matrix include actinides: Np, Pu, Am, Cm; lanthanides: La, Ce, Pr, Nd, Pm, Sm, Eu, Gd, Y; and Sr, Zr, Ba, Te, Nb within the limits of their solubility in UO_2 and to the extent

* Corresponding author. SKB, Box 3091, SE - 169 03, Solna, Sweden.
E-mail address: kastriot.spahiu@skb.se (K. Spahiu).

https://doi.org/10.1016/j.jnucmat.2019.151981

that they have not precipitated in perovskite-type oxides. The fission and activation products that form under irradiation in the reactor may stay in the locations where they are produced, or migrate depending on their solubility in the UO_2-matrix. Fission products that have limited solubility in the UO_2-matrix usually segregate to the grain boundaries during restructuring by thermal diffusion.

The release of toxic and radioactive species from spent fuel in contact with water is expected to depend mainly on the dissolution rate of the UO_2-matrix, since the great majority of radio nuclides (>90%) are preserved in the fuel matrix [5]. Within a few years after closure of the repository, all the oxygen present will be consumed by reducing minerals and bacteria, resulting in oxygen free and reducing environment [6,7]. Under these conditions $UO_2(s)$ is stable and the release of actinides and the majority of fission products will be controlled by its low solubility. However, the rate of dissolution is strongly influenced by the chemical conditions. In an oxidizing environment, the solubility of UO_2 increases by several orders of magnitude by the oxidation of U(IV) to U(VI) [8]. The groundwater composition as well as its pH can alter the dissolution rate. Physical features such as grain size, structure, cracks, porosity in the UO_2-matrix and the surface area in contact with water as well as temperature will affect the reaction rates as well as the radionuclide solubilities. Both, the dissolution rate of the spent fuel itself, and the release/retention of radionuclides are expected to be governed more by geochemical constraints encountered in the near field of the waste package, rather than by inherent material properties of the fuel. Conditions such as the redox potential and the pH of the solution as well as the availability of oxidative radiolysis products are key parameters controlling the overall alteration behavior of spent fuel.

The spent fuel generates a complex radiation field (α, β and γ) with broad energy spectra due to the decay of unstable nuclides. Spent fuel in contact with water will produce very reactive radicals ($OH\bullet$, $H\bullet$, $OOH\bullet$, e^-_{aq}) and molecules (H_2O_2, H_2, O_2) due to radiolysis of water [9]. Although oxidizing and reducing radiolytic species are produced in equivalent amounts, the lower reactivity of the molecular reducing species (mainly hydrogen) will lead to locally oxidizing conditions near the fuel surface. In order to understand and model spent fuel alteration/dissolution it is necessary to consider these oxidants in the mathematical models used to describe the near field. The effects of α-radiolysis are considered as dominating, both because of the much longer time periods of its presence, and because of the short range from the fuel surface in which the energy is deposited.

If the spent fuel comes into contact with water, the release of actinides and most of the fission products will depend on $UO_2(s)$ matrix dissolution and corrosion processes. Transport by groundwater is the only credible mechanism for migration of radionuclides contained in the spent fuel to the biosphere. Migration is only possible in case of a damaged canister; it is then important to evaluate the rate of dissolution of the spent fuel matrix and the rate of release of the various radionuclides, the so-called source term. In this evaluation it is important to consider both the effects of radiolytic oxidant production and the role of dissolved hydrogen and Fe(II) ions produced by iron corrosion.

In most deep repository concepts [10,11] relatively large amounts of dissolved hydrogen will be present during long time periods. A major hydrogen source is the anoxic corrosion of the massive iron containers:

$$3Fe(s) + 4H_2O \Leftrightarrow Fe_3O_4(s) + 4H_2(g)$$

The equilibrium pressure of hydrogen for this reaction is very high, of the order of several hundred atmospheres [12]. Another hydrogen source is α-, β- and γ-radiolysis of the groundwater by the radiation of spent fuel.

In the Swedish and Finish concepts for disposal of high level waste, the spent nuclear fuel will be encapsulated in copper canisters with a massive cast-iron insert. In the case of a limited container defect and groundwater intrusion, the anoxic corrosion of iron gives rise to the production of hydrogen at a higher rate than its diffusive mass transport away from the canister. The concentration of dissolved H_2 in the solution inside the canister is expected to quickly exceed its solubility in groundwater [13,14]. Gas phase formation occurs when the pressure of the hydrogen equals at least the hydrostatic pressure, around 5 MPa at 500 m depth. For this reason, it is considered relevant to study spent fuel leaching in the presence of hydrogen at pressures up to 5 MPa, corresponding to dissolved H_2 concentrations of ~40 mM.

At the range of temperatures expected in a repository (<100 °C) in spite of being a potential reductant, dissolved hydrogen is kinetically hindered in the absence of catalytic surfaces [2] and is not expected to contribute in the redox capacity of the deep groundwaters. However, the results of several published studies in recent years show a large impact of the presence of dissolved hydrogen in suppressing effectively the radiolytic fuel oxidation/dissolution process. Very low and practically constant concentrations of all radionuclides were observed during more than a year-long studies of spent fuel powder leaching in synthetic granitic groundwaters [15,16] under 5 MPa hydrogen pressure. Decreasing rates of radionuclide releases were observed in 5 M NaCl [17,18] under 3.2 bar H_2 with a clad fuel pellet and in synthetic granitic groundwater under 0.5 MPa H_2 with fuel powder [19]. Results of fuel fragment leaching in simulated granitic groundwaters are available also for high burnup fuel [20] and for MOX fuel, which has a much higher alpha radiation field [21]. In particular, very strong effects on reducing the matrix dissolution rates and immobilization of important radionuclides were observed during a long-term test of simultaneous corrosion of spent fuel fragments and metallic Fe powder in simulated granitic groundwater under Ar atmosphere from start [22]. A similar test in 5 M NaCl brine with a clad fuel pellet, where a final partial pressure of 2.8 bar H_2 built up in the autoclave [23,24] indicated decreasing and low actinide concentrations, but also a continued slight release of Sr and Cs.

In another study [25] of spent fuel dissolution rates in solutions saturated with hydrogen at 1 atm. by using a flow-through technique, a decrease of the dissolution rates of the spent fuel by 3–4 orders of magnitude as compared to dissolution under oxidizing conditions was observed.

One of the objectives of this study was to confirm the results obtained during the flow through tests under stationary conditions, with exactly the same fuel, the same simplified groundwater composition, hydrogen concentration and temperature as reported in Ref. [25]. It was discussed that under 1 bar hydrogen and room temperature it is difficult to avoid oxidized uranium in solution [26]. The two previous fuel leaching studies at Studsvik under 5 MPa [15,16] or 0.5 MPa [21] were carried out at 70 °C from start and the temperature was lowered only towards the end of the test. Here we started at room temperature in both autoclaves. The presence of steel surfaces in the previous autoclave leaching experiments was considered as a potential factor to affect the results [17]. For this reason, special care was taken to avoid any contact of the leaching solution with metallic parts of the autoclave and in one test even the gold basket used to insert the fuel was substituted by a quartz vessel with glass filter bottom. A solution sample was analyzed for traces of Fe(II) and they were found below the detection limit of ICP-MS(~1 ppb), thus excluding any Fe(II) influence in the interpretation of the results.

Another aim of the present study was to test spent fuel leaching

in the presence of hydrogen investigating the influence of various factors such as fuel surface area, leaching temperature and hydrogen pressure. The radiolytic oxidants are produced continuously during the several months (years) experiments and no observable quantities of oxygen, hydrogen peroxide or oxidized radionuclides are detected in the autoclave. In order to find out if they cause any surface oxidation of the fuel, an investigation of the oxidation state of the fuel surface by X-ray Photoelectron Spectroscopy (XPS) was carried out after the tests. This required special care to avoid any oxidation of the fuel surface by air during autoclave opening and fuel grain transport to the XPS apparatus, given the high sensitivity of the UO_2 surface to traces of oxygen [27]. In this investigation, the 4f spectrum of uranium was measured for detecting any potential oxidation of the surface as well as before and after the leaching of the fuel surface.

2. Experimental

Two experiments (denoted 4U6 and 5U1) were carried out in quartz lined stainless steel autoclaves manufactured by Métro Mesures. The volume in each autoclave was 1.2 dm^3. The autoclaves were thermostat controlled and equipped with pressure gauges, inlet and outlet tubing for pressurizing and sampling. Both gas samples and solution samples were collected regularly while the experiments were ongoing. In one of the autoclaves (4U6), the spent fuel sample (~1.8 g) was placed in a small gold net basket with a gold net cover to avoid the escape of fuel particles into the leaching solution. In the other autoclave (5U1) the spent fuel sample (~2.0 g) was placed in a quartz tube with a frit filter bottom, to avoid stationary solution in contact with the spent fuel. The sample holders were situated in the centre of the autoclaves. The quartz tubes for solution sampling had internal glass frit filters to avoid escape of fines in the solution samples from the pressure vessels. This avoids any oxidative dissolution of fines during filtration or ultracentrifugation ex-situ. A PEEK drop collector placed at the internal surface of the autoclave lid avoided any contact of condensed vapor with the steel surfaces.

2.1. Fuel

The spent fuel samples in experiment 4U6 were taken from a sieved fraction in the size interval 250–500 μm that originated from a PWR fuel rod irradiated for 5 cycles to a calculated rod average burnup of 41.3 MW d/kg U, which has been well characterized [28,29]. The spent fuel samples in experiment 5U1 were taken from a sieved fraction in the size interval 2–4 mm that originated from a BWR fuel rod irradiated in the period 1972–1978 to an average rod burnup of 42 MW d/kg U [30]. The local burn-ups (as determined by Cs-137 γ-scanning and Nd-148 chemical burn-up) were 43 MW d/kg U and 42 MW d/kg U, respectively. The spent fuel fragments were pre-leached in a solution of the same composition as the leaching solution under purging of Ar + 10% H_2 + 0,03% CO_2 during 24 h in order to dissolve most of the instant release fraction and any potential pre-oxidized layer on the fuel fragments.

2.2. Leaching experiments

In the experiments, 950 ml leaching solution (10 mM NaCl, 2 mM $NaHCO_3$) was introduced into each autoclave at room temperature; the solutions were then purged with Ar for approximately 18 h before introducing the spent fuel samples and pressurizing. In autoclave 4U6 (Ar + 10.3 mol% H_2) at 10 bar was introduced and the temperature was set to 25 °C. In autoclave 5U1 pure H_2 at 5 bar was introduced and the temperature was set to 25 °C. Due to technical problems with sampling and air leakage into autoclave 5U1, the autoclave was re-pressurized after 17 days.

Approximately 10 ml solution samples were extracted from each autoclave at different time intervals and analyzed with ICP-MS (ELAN DRCII) in three parallel samples. The solution samples were weighed with 0.1 mg precision and the remaining solution volume in the autoclave could thus be calculated (e.g. 843.46 ml at the end of 4U6 test). The first sample was used for Cs-137 determination by γ-spectroscopy, while the two others for ICP-MS analysis. 15 ml samples were used for determination of total carbonate and pH in the beginning and at the end of the experiment. In most cases, gas samples were collected prior to solution sampling in order to determine the gas composition. The pressure was readjusted after each sampling by introducing new gas in the autoclaves. After a period of 487 days the gas composition was changed to pure H_2 at 50 bar in autoclave 4U6. After further 273 days the temperature was raised to 70 °C. In autoclave 5U1 the temperature was raised to 70 °C after a period of 432 days, the temperature was again set to 25 °C after further 301 days. The pressure was set to 5 bar H_2 throughout the experiment.

2.3. Analytics

The concentration of fission products and actinides were measured with ICP-MS. All samples contained 1% HNO_3 and 1 ppb In-115 as internal standard. Measurements in the mass range 80–254 amu were carried out. Sensitivity factors for the different elements relative to In-115 were calculated by a one-point calibration using multi-element standards. Nuclide concentrations were calculated by relating the signals to the In-115 signal. Further details on ICP-MS analysis may be found in Ref. [25]. The detection limit is ppt (ng dm^{-3}) and the quantification limit is ppb (μg dm^{-3}), with an error limit ~20%. Prior to ICP-MS analysis, the Cs-137 concentration was measured with γ-spectrometry. A one point calibration was made with a 1.8 MBq (~31 ppb Cs-137) solution. All samples were measured for 30 min.

It is customary in spent fuel dissolution studies [31,32] to report the FIAP (Fraction of Inventory in the Aqueous Phase) for fission products such as Cs, Sr, I and Mo. FIAP is expressed as the ratio of the inventory of a given nuclide in the aqueous phase to that of the inventory of the same nuclide in the solid fuel sample:

$$FIAP(X) = (C_x\ AM_x\ V_{soln})/(m_{fuel}\ f_{HM}\ Xf_x) = A_x\ V_{soln}/(m_{fuel}\ f_{HM}\ Af_x)$$

where C_x is the concentration of the radionuclide X in solution in mol/L, AM_x is its atomic mass, V_{soln} is the volume of the solution (L), including the volume of the sample taken for analysis Vs, m_{fuel} is the mass(g) of the fuel sample in contact with the solution, f_{HM} is the fractional mass of heavy metal in the fuel, Xf_x is the specific inventory of radionuclide X in solid fuel (g/(g HM)), A_x is the specific activity of the radionuclide X in solution (Bq/L) and Af_x the specific radionuclide inventory (Bq/(g HM)) in the solid.

An average fractional release rate ($FRR_n(X)$, units d^{-1}) during the time interval between two samplings at t_n days and t_{n-1} days may be determined from the difference between the corresponding cumulative fractional releases:

$$FRR_n(X) = [CumFIAP_n(X) - CumFIAP_{n-1}(X)]\ /(t_n - t_{n-1})$$

$$FRR_n(X) = FIAP_n(X) - FIAP_{n-1}(X)(1-V_{s,n-1}/V_{tot,n-1})$$

Gas samples were collected and analyzed with Gas-MS (Fisons VG Gas Analysis System Ltd, MM8-80S, detection limit of 50 ppm) and GAM 400 (detection limit of 1 ppm) to ensure that there were no traces of air in the autoclaves at the beginning of the

experiments.

2.4. XPS analysis

The H_2 pressurized autoclave which contained the smaller particles (4U6) was moved to an Ar-glove box by taking away its back side and placing it back after autoclave insertion. After allowing enough time to pass until all traces of oxygen introduced with autoclave insertion disappeared, with the help of the Cu-catalyst, the autoclave was opened inside the glove box and a few fuel fragments were taken out from the gold basket. The fragments were immediately dried under a halogen lamp in order to avoid oxidation of the surface due to radiolytically formed H_2O_2 and O_2. One of the fragments was washed with Milli-Q water to get rid of possible salt deposits from the leaching solution and the fuel fragment was once again dried under the halogen lamp. One reference fuel fragment that had not been in the autoclave but originated from the same fuel and sieving batch (blank sample referred to as particle 1), one leached and washed fuel fragment (particle 2) and one leached but unwashed fuel fragment (particle 3) were prepared onto an indium foil, which was mounted on a sample holder for XPS analyses. The vacuum transfer vessel (PHI, model 04–110) containing the sample holder was placed inside an additional gas tight container in order to avoid intrusion of air traces (read O_2) to the three fuel fragments during transport. The fuel fragments were introduced into the UHV of the XPS (Physical Electronics Inc. (PHI), model 5600ci) avoiding any air contact.

The spectrometer was equipped with a monochromatic Al K_α X-ray source ($h\nu$ = 1486.7 eV). The monochromator was double focusing with a spot size on the sample of approximately Ø 0.8 mm. Thus, by use of the monochromator, subsequent analyses at several spots or samples were possible without irradiating the whole sample holder.

Survey scans were recorded with an X-ray source power of 200 W and pass energy of 187.85 eV of the analyser. Narrow scans of the elemental lines were recorded at 11.75 eV and 23.5 eV pass energy which yields an energy resolution of 0.60 eV and 0.73 eV FWHM respectively at the Ag $3d_{5/2}$ elemental line of pure silver. Calibration of the binding energy scale of the spectrometer was performed using well-established binding energies of elemental lines of pure metals (Cu $2p_{3/2}$ at 932.62 eV, Au $4f_{7/2}$ at 83.96 eV) [33]. Errors in binding energies are typically ±0.1 eV for metals and ±0.2 eV for isolators. The samples were conductive with O 1s elemental line of oxide at 530.2 eV binding energy. Data analysis was performed using PHI MultiPak program. Secondary electron images were recorded by use of the electron gun (10 kV) of the Auger option.

3. Results and discussion

In this section the results of the analysis of the fuel leaching behaviour in both autoclaves are presented. In the first part the evolution of the concentrations of actinides, lanthanides and Tc with time is discussed, coupled with the potential fate of the molecular radiolytic oxidants. In the second part, the release of non-redox sensitive radionuclides such as Cs and Sr is discussed through their FIAP (Fraction of Inventory in the Aqueous Phase) and FRR (Fractional Release Rate). In both parts the data are compared with similar tests published before and discussed.

3.1. Results of the spent fuel leaching under 1 bar H_2-Autoclave 4U6

3.1.1. Actinides, lanthanides and Tc

The interpretation of the data on spent fuel leaching is usually based on the measured concentrations of the radionuclides released from the solid fuel at different sampling times during the duration of the test. The results of the evolution of the ICP-MS measured concentrations for a few actinides, lanthanides, and ^{99}Tc with time during the leaching of spent nuclear fuel fragments (⌀ 0,25–0.5 mm) in 10 mM $NaHCO_3$ and 2 mM NaCl under starting conditions 25 °C and 1 bar H_2 (experiment 4U6) are presented in Fig. 1.

As noted in Fig. 1, the concentration of U, which is the main component of the fuel matrix, decreases steadily from start, and a similar behaviour is noted for Np. This is in fact quite an unexpected result, because what happens usually during fuel leaching in carbonate solutions in absence of added hydrogen is that the concentration of U increases quickly due to the oxidation of the fuel surface by the radiolytic oxidants and new amounts of soluble uranyl (U(VI)) compounds are produced from the oxidation of the U(IV) of the fuel matrix. In our case a decrease of the concentrations of uranium in solution from ~3×10^{-7} M at start to ~2×10^{-9} M after 487 days is observed. A similar behaviour has been observed in several other fuel leaching tests under hydrogen atmosphere [16–21]. This indicates that uranyl carbonate species, originating from a pre-oxidized layer in the fuel, are reduced and precipitated as UO_2 (am). Alternative explanations, such as e.g. precipitation of any U(VI) solid can be ruled out, based on the following reasoning. Sometimes it is discussed that, since the radiolysis continues to produce oxidants all the time, maybe some precipitate of U(VI) compounds forms on the fuel surface and this is difficult to detect, because the fuel surface not always is investigated with surface sensitive techniques, as done in these tests. During the long duration of fuel tests (several months to years), we view it as impossible that any potential U(VI) solid formed does not equilibrate with the solution, i.e. does not release U(VI) in solution corresponding to its solubility product. The U(VI) solid expected to form under the present conditions is schoepite (uranyl hydroxide), having almost a 10^{-3} M solubility under our conditions, i.e. the total uranium concentrations in solution would be almost one million times higher in its presence. In general, U(VI) solids are much more soluble than UO_2(s). Among the most insoluble U(VI) solids expected to form during fuel leaching tests are Ca-uranyl-silicates, such as uranophane [34], which still has a solubility about two orders of magnitude higher than UO_2(s) at near neutral pH. We have not introduced Ca in our solutions, and the corresponding Na compounds are more soluble.

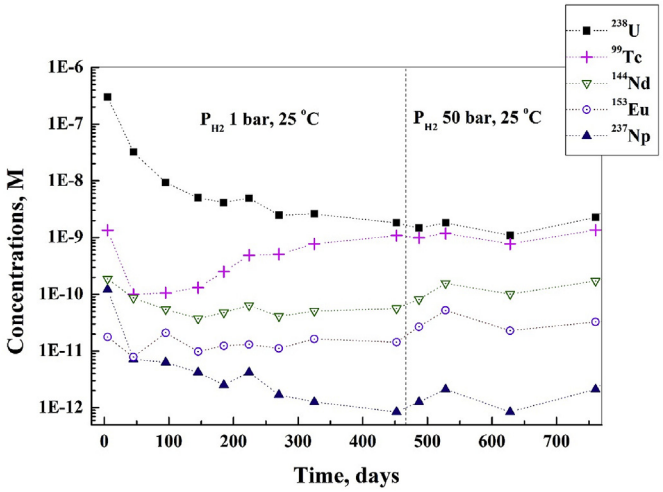

Fig. 1. Evolution of the concentrations of actinides, lanthanides and Tc in autoclave 4U6. The concentration of U, Np, Nd, Eu, and Tc is plotted as a function of leaching time. Spent fuel fragments: ⌀ = 250–500 μm. Starting conditions: P_{H2} = 1 bar, T = 25 °C.

During leaching under aerated conditions in distilled water, uranyl peroxide solids such as studtite and meta-studtite have been reported to form both during leaching of spent fuel [35–37] and UO_2 irradiated with accelerator α-particles [38], or simply by adding hydrogen peroxide to UO_2(s) [39–41]. However, in the presence of carbonate in the leaching solution both in the case of spent fuel [36] and UO_2(s) [40], studtite or metastudtite was not observed, probably due to the high stability of the uranyl carbonate complexes, which decrease very much the concentration of free uranyl ions in solution. Further, the very low concentrations of uranium measured at longer times in our test indicate that uranium is mainly present as U(IV). This would not be possible if traces of hydrogen peroxide existed in the solution, given its very fast reaction with U(IV) at the pH of our solutions [42,43].

The pre-oxidized layer contributes also to the initial increased releases of ^{90}Sr, ^{137}Cs and ^{100}Mo, as discussed later. Carbonate forms strong complexes with uranyl ions under our experimental conditions; the predominating U(VI)-species are $UO_2(CO_3)_2^{2-}$ and $UO_2(CO_3)_3^{4-}$ [8]. Despite the pre-leaching of the fuel fragments, there is still a pre-oxidized surface layer, as can be judged from the starting concentration of [U] ~ 3×10^{-7} M.

It should be kept in mind that this reductive precipitation occurs in the presence of the very strong radiation field of the spent fuel a few years after discharge, composed of a high α-field (dose rates of the order of 1500 Gy/h) affecting a 30–40 μm water layer near the surface and a β-field with ranges up to 1 mm in water, while the γ-field affects the whole volume of the test solution.

Dissolved H_2 acts through a well-known mechanism for radical rich (low LET) β- and γ-radiation in homogeneous solutions, by scavenging the oxidizing OH-radical [44,45]:

$$H_2 + OH = H_2O + H \quad k = 4 \times 10^7 L\ mol^{-1}s^{-1}$$

This interaction converts the strongly oxidizing OH-radical into water and the reducing H-radical (atomic hydrogen), causing thus a general decrease of the concentrations of the oxidizing radical and molecular species. In any case, given that the molecular oxidizing species (H_2O_2 and O_2) are very active towards e.g. U(IV) in solution or in the solid phase, while the reducing molecular species (H_2) is considered inert at low temperatures, the radiolytic modelling of the whole system predicts only a slower oxidation of the fuel matrix [46] if one does not consider any effect of the fuel surface.

Usually not all of the H_2O_2 produced near the spent fuel, mainly by α-radiolysis, reacts with its surface: a part diffuses away and the same holds for molecular oxygen. It has been shown lately in experiments with SIMFUEL [47] that more than 99% of the added H_2O_2 was decomposed catalytically at the fuel surface into water and oxygen. Similar experiments with SIMFUEL and added H_2O_2, but in the presence of 10 bar D_2 [48] showed that a large part of the peroxide reacted with D_2 to give water, another large part was decomposed to water and oxygen and only less than 0.02% of the peroxide produced U(VI).

Direct measurements of the O_2 will be described later in section 3c. However tests of spent fuel leaching in the presence of 0.8–43 mM dissolved H_2 [18–22,49] indicate oxygen levels below the detection limit (less than 10^{-7}-10^{-8} M). Another indication that the levels of molecular radiolytic oxidants are extremely low comes from the low U concentrations (below $10^{-8.5}$ M), indicating uranium presence mainly in the tetravalent state. It is well known that U(IV) in solution is stable only for extremely low O_2 fugacities [50], due to its very fast reaction with O_2 at room temperature [51,52]. It is generally accepted that H_2 does not react with H_2O_2 and O_2 at room temperature, thus the extremely low concentrations of molecular radiolytic products observed under these tests are mainly due to surface-mediated processes.

After 487 days the U concentration has decreased to ~2×10^{-9} M, the same levels as in previous studies under H_2 atmosphere [16,19]. This behaviour is typical for all tests carried out under hydrogen concentrations >1 mM [53]. These low concentrations of U in the leaching solutions are in good agreement with the solubility of $UO_{2(am)}$ [8].

The solid state chemistry of U(IV) is much simpler than that of U(VI): besides UO_2(s), only coffinite $USiO_4$(s) is known to form under hydrothermal conditions and then only at relatively high silicate concentrations.

The evolution of the concentrations of U, Tc, Np decreasing during the whole test seems to rule out any oxidative dissolution of the fuel. It is highly probable that the reduced Np(V) as Np(IV)-oxide co-precipitates with U(IV)-oxide. This is because the reported solubility of NpO_2(s) [8,54] is ~3×10^{-9} M, quite similar to this of amorphous UO_2 [8], while Np concentrations in solution are about three orders of magnitude lower than those of uranium, in line with the roughly 1000 times lower Np inventory in the spent fuel. This indicates a potential co-precipitation of NpO_2(s) with UO_2(s) as reported in the literature [55]. Also the initial (~100 days) concentration decreases for Nd and Tc may be due to co-precipitation-sorption processes of these nuclides to the newly formed solid phases. In any case, the total concentrations of the lanthanides are extremely low. They do not seem to correspond to the equilibrium concentrations of any lanthanide solid phases which could form in our solutions.

The reduction rate of U is considerably slower as compared with previous studies [18,19] at 70 °C and higher partial pressures, as will be discussed later.

After running the test for 487 days and 25 °C, only small changes are observed in the measured concentrations between 300 and 487 days. The gas atmosphere was changed to pure H_2 and the pressure was increased to 50 bar. We had already data for this H_2 concentration [18], but at higher temperature. Except for a slight increase of some redox sensitive radionuclide concentrations due to the unavoidable air contamination, the steady state values did not differ considerably from those at 1 bar.

However there was considerable pressure loss during this period: it seems that the packing made of Viton leaked more under the effect of age and radiation and the leakage became even worse later when the temperature was raised to 70 °C.

3.1.2. *Release of non-redox sensitive fission products such as Cs and Sr*

Most of the previous experience is based on fuel leaching tests carried out in the presence of air and accompanied with substantial U(VI) releases, with the potential formation of a variety of U(VI) secondary phases, depending on the composition of the leaching solution. For this reason it was unreliable to analyse fuel dissolution using uranium releases and methods to evaluate fuel dissolution based on the release of fission products such as Sr were elaborated [31,32]. Usually the analysis of fuel dissolution is based on the evolution of FIAP (Fraction of Inventory in the Aqueous Phase) with time, shown in Fig. 2 for autoclave 4U6.

We have included also Cs and Mo, given that Mo is released from fuel as molybdate (MoO_4^{2-}), which seems kinetically stable under our conditions (see also the quite constant Mo levels in Fig. 4). For the first time in these experiments we observed measurable levels of mass 90 in the leaching solution (10 mM NaCl and 2 mM $NaHCO_3$) before introducing the fuel sample, which apparently are due to ^{90}Zr released from the glass liner in the autoclave or some other source of ^{90}Zr contamination. They were relatively low and do not seem to have affected much the FIAP analysis for ^{90}Sr in this test, while the situation is different for the 5U1 autoclave, see further. Nowadays one can analyse these isobars at Studsvik with the

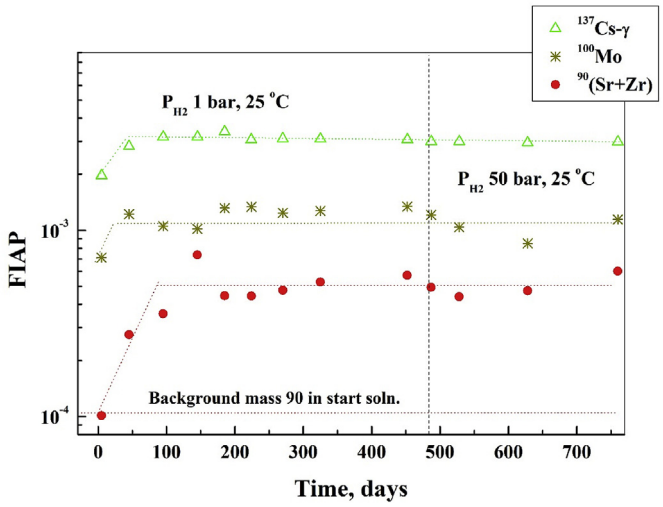

Fig. 2. Autoclave 4U6. FIAP of Cs measured by γ-spectrometry, (Sr + Zr) and Mo is plotted as a function of leaching time. Starting conditions: p_{H2} = 1 bar, T = 25 °C.

collision chamber ICP-MS, but this was not possible when these tests were carried out. We have used ^{137}Cs data as measured by γ-spectrometry here and in other FIAP plots as more reliable, instead of those measured by ICP-MS, based on previous experience at Studsvik [56].

As seen from Fig. 2, a clear increase of the FIAP is noted immediately after start, due to the dissolution of the pre-oxidized layer. This conclusion is supported by the increase of FIAP of all fuel components, including typical matrix bound fission products or actinides. The FIAP levels in Fig. 2 become stable with time, showing that no further release from the fuel matrix occurs. In the case of fuel leaching under oxidizing conditions, sometimes the slope of the FIAP evolution with time is used to estimate the fuel dissolution rate [31,49]. In fuel leaching studies with hydrogen present, it seems that this method cannot be used.

A better analysis of the releases during the leaching is obtained using the Fractional Release Rates (FRR) for a time interval between two samplings, since the volume of the solution sampled is accounted for in the calculation of the FRR(t). In Fig. 3, the Fractional Release Rates (FRR(t) = FIAP/day) for Cs, (Sr + Zr) and Mo

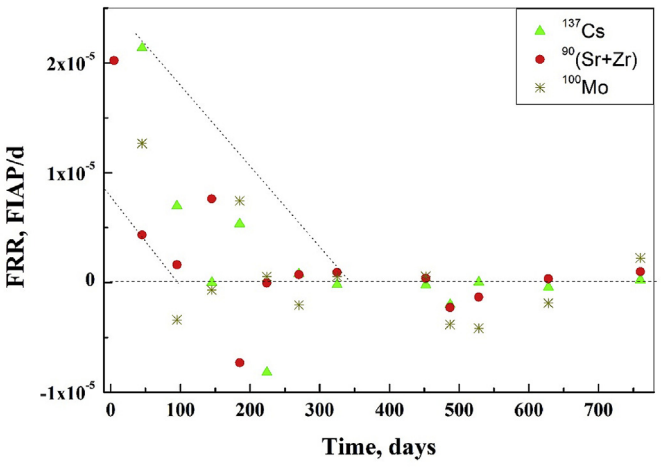

Fig. 3. Fractional release rates at each interval for Cs, Sr and Mo during autoclave 4U6 leaching. Note the several negative values obtained after ~100 days and the general decreasing trend during the first 350 days.

show a systematic decreasing trend with time during the first year of leaching.

The analysis of these data shows also that one never observes very low fractional release rates of the order of 10^{-9} FIAP/day. The positive FRR data are of the order of 10^{-5} to 10^{-7} FIAP/day but in many alternate intervals they become negative. This is mainly due to the fact that we have a small amount of fuel with relatively high surface area and low fractional release rates are usually obtained with large fuel samples of low surface area. Thus potential errors in solution volumes and especially the 20% error in the ppb or sub-ppb concentrations of most nuclides cause quite large errors in the calculated FRR data and they are discussed only qualitatively here.

In spite of this, both the decreasing trend of the FRR(t) during the first year for all three nuclides analyzed and the many intervals with negative FRR(t) are in line with the behavior of U and other nuclides discussed in section 3a1.

The use of ^{90}Sr as an indicator of the matrix dissolution under the conditions of our autoclave may be affected by the fact that the total amount of ^{90}Sr released during the whole leaching period corresponds to less than the amount of Sr contained in a monolayer of fuel surface [19,49]. The analysis of Sr releases is a well-established method for the oxidative dissolution of fuel, where several layers of matrix are altered during the period in which rates are analyzed. The effect of the hydrogen pressure and temperature on Sr releases may have different explanations, but it seems that under these conditions the FRR(t) of Sr are rather high especially at the beginning. They are lower towards the end of the leaching, especially at 50 bar and when lowering the temperature to 25 °C. Therefore it seems not probable that they are coupled to an oxidation-dissolution of UO_2. These Sr releases are probably due to the dissolution of Sr-containing perovskite type phases in grain boundaries or matrix surface reduction making Sr more easily released from the solid [57]. Both these phenomena are expected to contribute to a Sr release limited in time, and this is supported by the data on the continuation of the leaching at 50 bar after adding new solution to the autoclave containing the same fuel sample. These data were reported in Ref. [58], where the term “hydrogen memory” was used for the first time. In this case the releases of both Cs and Sr decrease with time and it seems that the fuel is not releasing any more Sr since too many negative FRR(t) values were obtained, even under Ar atmosphere [49,58].

Another interesting observation concerning Sr and Cs releases during fuel leaching in presence of hydrogen (added or produced in the autoclave by Fe(s) corrosion) comes from a series of experiments carried out at INE, Karlsruhe [16,17,23,24,49,59]. When the fuel sample was a whole fuel pellet together with cladding, a contradictory behavior of the actinides and redox sensitive elements as compared to Sr and Cs releases was observed both during leaching in presence of 8 g metallic Fe powder and with 3 bar hydrogen overpressure. The concentrations of U, Np, Tc and other redox sensitive nuclides decreased with time, approaching levels corresponding to the solubility of their tetravalent oxides. At the same time, a measurable increase of both Sr and Cs levels was observed. This was not the case in tests carried out under similar conditions in other laboratories, but with fuel fragments or fuel powder [15,16,19–22]. The same holds for a fuel slice leaching carried out later at INE [59], where a concordant behavior of the redox sensitive element behavior and Sr and Cs releases was observed. We consider possible that the continuous Sr and Cs releases in the case of the leaching of the high burn-up fuel pellet together with cladding originated very probably from the closed gap of the pellet, which may take years to get completely wetted [56] and in the process releases considerable amounts of Sr and Cs.

As discussed before, the pressure was raised to 50 bar after 487

days and in the last period the temperature was also raised to 70 °C. There was considerable pressure loss during this period due to the effect of aging and radiation on the packing made of Viton and leakage became even worse later when the temperature was raised to 70 °C. The air leakage is quite visible in the increase of the release rates during the last interval, contrary to the previous behaviour with alternating negative releases.

3.2. Release of radionuclides from 4d-metallic particles

Usually the radionuclides contained in the 4d metallic particles or ε-particles are discussed as potential contributors to the Instant Release Fraction (IRF), because they are present inside the grains, but mainly at the grain boundaries, thus outside of the fuel matrix. In all the tests carried out with spent fuel dissolution in the presence of hydrogen, the behaviour of fission products contained in the 4d-particles or ε-particles has never been reported. We considered doing this for those experiments, and in Fig. 4 the evolution with time of the concentrations of a few radionuclides expected to be contained mainly in the metallic particles is presented.

As seen from the figure, the concentrations of the radionuclides contained in the metallic particles and Mo, which is present both in the matrix and in ε-particles, remain quite low and constant during the whole leaching period. There seems to be a slight increasing trend up to ~500 days for most of them, but afterwards follows a slight decrease and the whole variation is in a very narrow concentration interval, e.g. 1×10^{-10} - 5×10^{-10} M, so they remain practically constant during the more than 2 year long leaching experiments.

The concentrations of all the other isotopes (except Mo, which is higher) are stable in the interval 1×10^{-10} - 5×10^{-9} M. In spite of the paucity of the chemical data for these noble metals, these steady state concentrations are lower than the expected solubilities of their corresponding oxides [60]. Thus the concentrations of Pd in equilibrium with PdO_2(s) would be ~3×10^{-6} M while those in equilibrium with Pd(s) < 10^{-15} M. In a comparison of the concentrations of silver in groundwaters to the much lower ones resulting from equilibrium calculations with metallic silver under reducing conditions (less than 10^{-13} M for $E_h = -0.2$ V in 0.1 M NaCl solution at 25 °C), it was proposed that this was due to the absence of the equilibrium between metallic silver and dissolved atomic silver Ag(aq) in the thermodynamic databases [61]. Two experimental studies [62,63] which have investigated this equilibrium have determined constants that would result in silver concentrations ~6×10^{-9} M respectively ~3×10^{-7} M under reducing conditions. We were not able to find any corresponding data for Pd(aq), Rh(aq) or other components of the metallic particles in the literature and we can only report the measured concentrations in solution when metallic particles contact the solution for more than 2 years. These concentrations are orders of magnitude higher than those calculated from equilibrium with the corresponding metal under reducing conditions and much lower than those calculated in equilibrium with the corresponding oxide, but we have no basis to dismiss or confirm the hypothesis of dissolved metal atoms in solution.

During the leaching of synthetic metallic particles in air, Cui et al. [64] noted higher releases of the less noble metals, and the leach rates under oxidizing conditions followed the metal oxidation potentials, with releases decreasing in the order Mo > Tc > Ru ~ Rh ~ Pd. Similar results as in our tests were obtained with metallic particles extracted from spent fuel in the presence of 0.1 bar H_2 [65], with Mo concentrations dropping to sub-ppb levels in the presence of hydrogen. Albinsson et al. [66] report also constant Ru concentrations during spent fuel leaching in presence of hydrogen at the same concentration interval as in our test.

For this reason, the content of these isotopes is expected to remain practically unchanged in the metallic particles during the long periods of time in the repository and these isotopes can be accounted for in the criticality calculations even for long term fuel evolution.

A potential corroding agent for metallic epsilon particles in spent fuel is the sulphide or the arsenic of deep groundwaters, giving rise to the very insoluble metal sulphides or arsenides at the surface of metallic particles exposed to groundwater, as shown by natural analogue studies [67].

3.3. Redox conditions in the autoclave and air leakage

In Fig. 5, the concentration of O_2 and N_2 is plotted as a function of leaching time for autoclave 4U6. There are almost no measurable levels of O_2 during the first 487 days, indicating that the intruded O_2 (as judged from the increasing N_2 levels) must react and be consumed in the leaching solution or at the fuel matrix surface. However, there are no signs that the matrix has dissolved markedly, as in such a case the concentration of congruently dissolved species such as Sr and Cs would increase proportionally. The rate of U(VI) reduction may be affected by the influx of O_2, becoming slower

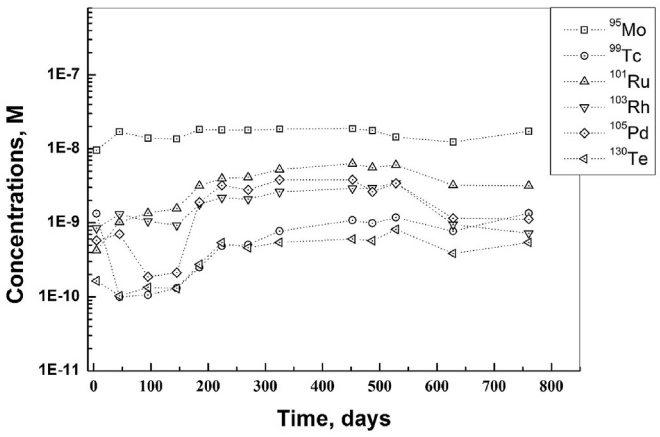

Fig. 4. Evolution of the concentrations of a few radionuclides contained in the ε-particles with time during fuel leaching under 1 bar H_2.

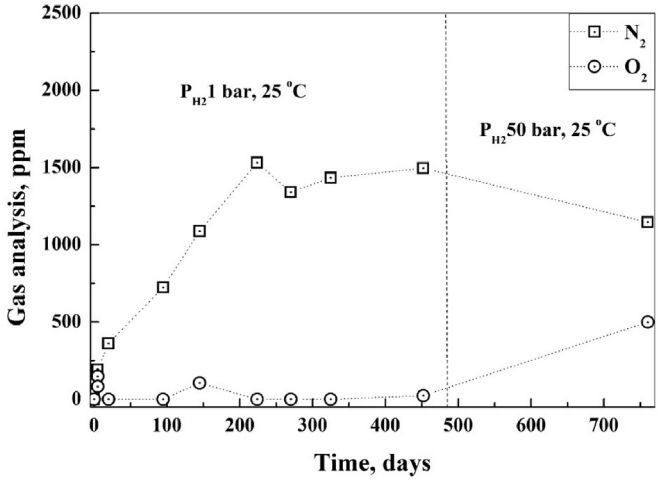

Fig. 5. Results of gas analysis in autoclave 4U6; levels of N_2 and O_2 as a function of time.

than in a purely reducing environment.

This means that the very low U and other concentrations were measured in presence of measurable air contamination, as can be seen from Fig. 5.

The gas sample on day 760 showed increased levels of O_2, see Fig. 5, after the gas change to 50 bar H_2. The gas pressure had decreased to 38.2 bar at the time of sampling. The leakage does not seem to influence the system significantly, the concentration of U remains at 10^{-9} M.

Anyhow, the concentrations of Tc would indicate a slight increase after the initial decrease and this may be due to its higher sensitivity to oxygen traces. This seems not to be the case for autoclave 5U1, where Tc concentrations decrease all the time, in spite of an apparently larger air leakage. The gas sampling indicates further air leakage into the autoclave, equivalent to the air intrusion at day 452, see Fig. 5. The gas pressure had decreased to 40.1 bar at the time for taking the last sample before finalizing the experiment.

An attempt to determine H_2O_2 concentrations as the experiment was completed showed concentrations below the detection limit (~10^{-7} M). Albinson et al. [66] have shown that precipitation of reduced U from the pre-oxidized layer occurs on the spent fuel surface itself. To confirm these studies, the quartz beaker was stripped with concentrated HNO_3 when the experiment was finished in order to do a mass balance of the leached nuclides. Since fuel fragments had escaped from the gold basket into the solution, a proper mass balance was not possible in our case.

3.4. XPS surface analysis

Fig. 6 shows the scanning electron images of the three analyzed particles (#1, #2 and #3, see Experimental part for their pretreatment). The surfaces of the samples appear free of secondary phases [68] and the grain boundaries exhibit no clear corrosion attack. Loose particles may have been washed off from the surface during preparation.

The XPS analyses show that the surface of the reference fragment (particle 1) contains predominantly uranium in the U(VI) state (Fig. 7). The U 4f spectra of leached fragments in the autoclave (particles 2 and 3) are almost identical and similar to pure UO_2 surfaces produced through breaking a virgin UO_2 pellet in the XPS apparatus under vacuum and measured with the X-ray monochromator at the same parameters (Fig. 8). The narrow scans of the U 4f elemental lines show U $4f_{7/2}$ at a binding energy of 380.1 eV and satellites with a spacing of 6.9 eV to the main lines, characteristic for UO_2 [69,70] (see Fig. 8).

The satellites of the U 4f lines of particles 2 and 3 are at the same position as the satellites of the U 4f spectrum of UO_2 but their intensity is slightly less, see Fig. 8. The results from XPS are in accordance with the leaching results. Fig. 1 shows U concentrations that derive from initial dissolution of the pre-oxidized surface layer

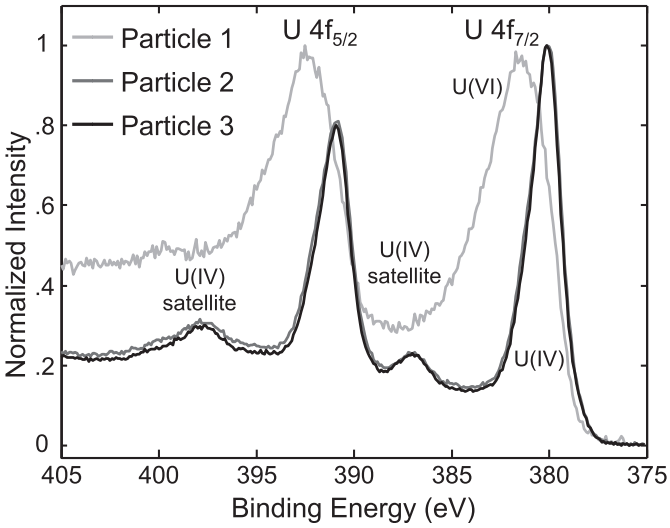

Fig. 7. Comparison of the U 4f spectra of the three samples (raw data). Al K_α monochromator. X-ray source power: 100 W, pass energy 23.5 eV.

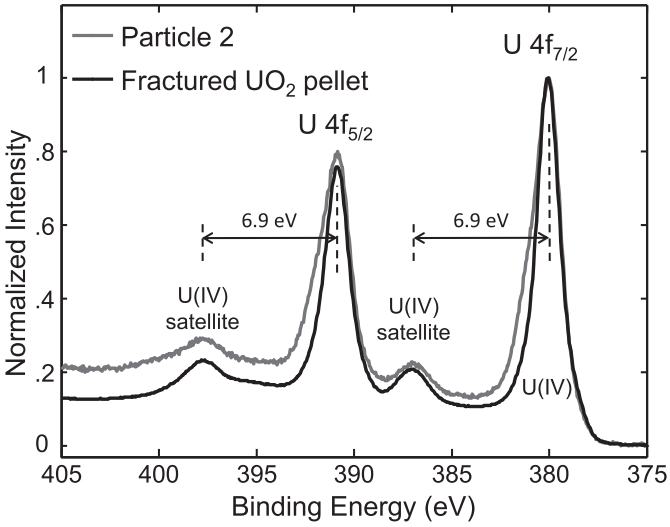

Fig. 8. Narrow scans of U 4f spectra of particle 2 and of a UO_2 pellet fracture scaled to similar intensity. A certified UO_2 pellet sample (IRMM No. CBNM) was fractured in the UHV of the XPS. Both spectra are measured by Al K_α mono excitation at same pass energy (11.75 eV).

which corresponds to the XPS data of the reference fragment (particle 1).

The difference in the XPS spectra of spent fuel particles with

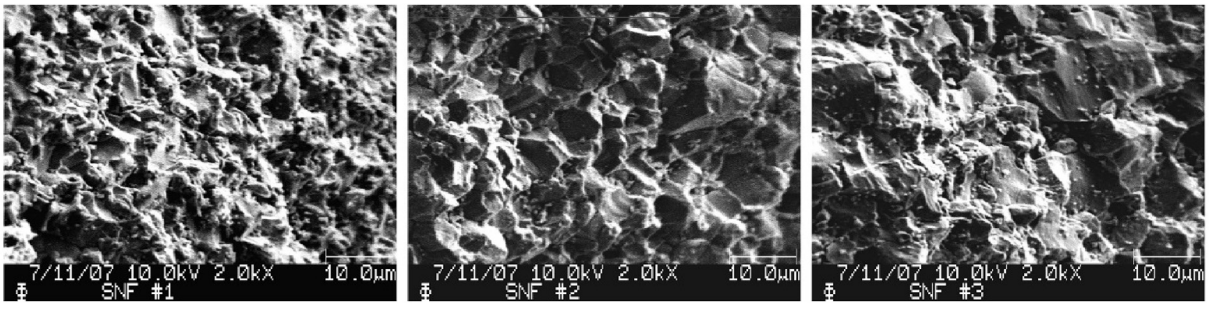

Fig. 6. Secondary electron images of the particles (#1, #2 and #3) from autoclave 4U6.

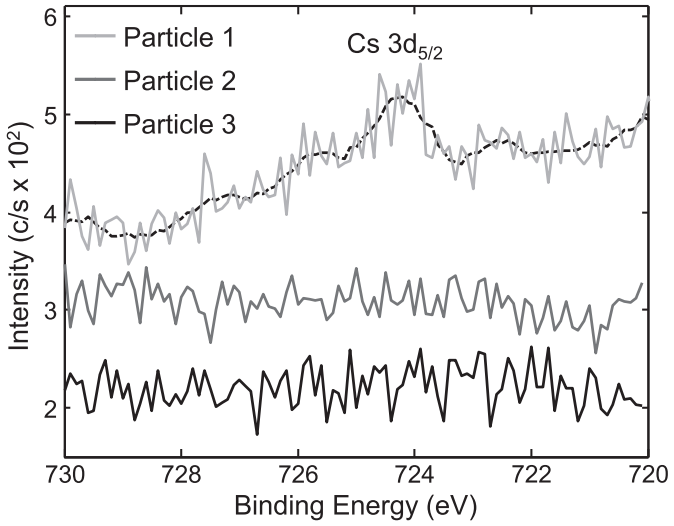

Fig. 9. Narrow scans of the binding energy range of Cs $3d_{5/2}$ elemental line. At the spectrum of particle 1, smoothed data are superposed as dotted line to guide the eye.

spectra of pure UO_2 is mainly due to the presence of non-uranium cations in the spent fuel. This becomes clearer by comparing with published XPS SIMFUEL spectra [71,72]. Santos et al. [71] fit the spectra of reduced SIMFUEL surfaces with a ~21% contribution of U(V) and ~11% contribution of U(VI), which is quite similar to our spectra for particles 2 and 3. In a series of publications, Prieur et al. [73–76] have used X-ray Absorption Spectroscopy in the High-Energy-Resolution Fluorescence-Detection mode (XAS-HERFD) and other spectroscopic methods to investigate La(III) or Am(III) doped UO_2. They conclude that during the substitution of U(IV) with La(III) or Am(III), the UO_2 fluorite structure compensates the incorporation of the aliovalent cation by the formation of U(V) in quasi equi-molar proportions.

The last sampling in autoclave 4U6 shows intrusion of air into the autoclave, resulting in increased levels of U and other radionuclides. However, the XPS analysis displays the presence of U(IV) on the surface of the leached fragments indicating that carbonate has effectively dissolved any U(VI) formed on the surface.

The role of carbonate in enhancing the dissolution rate of UO_2(s) and spent fuel, or in complexing the U(VI) in the surface and releasing it in solution has been discussed in several publications [5 and references therein]. However, the only quantitative XPS results on UO_2 leached in bicarbonate solutions of different concentrations are those of de Pablo et al. In the first publication [77] they report $UO_{2,05}$ at the surface during static leaching of UO_2 in the presence of 10 mM $NaHCO_3$, while a clean $UO_{2.0}$ surface is reported in experiments where the highest bicarbonate concentration was 50 mM [78]. The XPS analysis of an alpha doped UO_2 pellet leached in a solution with the same composition as ours and variable hydrogen concentration [79] reported $UO_{2.0,}$ i.e. a completely reduced surface.

In a previous study [53] it was observed that towards the end of the leaching period under 5 bar H_2, the FRR(Cs) are consistently negative, while the releases of Sr continue much longer. The XPS analysis here also shows that Cs exists on the reference fragment, but cannot be found on the fragments leached in the autoclave. One potential explanation could be that the leached fuel surface has been depleted of Cs, alternatively the fuel surface is covered with precipitated amorphous UO_2. An estimation of the thickness of this UO_2(s) layer assuming the precipitation of 65 μg UO_2(s) in autoclave 4U6, with density 10.5 g/cm^3 on the surface of 2 g fuel powder with a BET surface ~300 cm^2/g results in a uniform layer of ~0.1 nm, which attenuates the Cs 3d electrons by a factor of ~0.9 only.

As can be noted from Fig. 7, the XPS results show that the initial uranium derives from a pre-oxidized surface layer (particle #1). Cs was also found on particle #1 at trace level. The information depth (95% of signal) of the Cs $3d_{5/2}$ elemental line in UO_2 is 2.2 nm, calculated by the CS2 equation of Cumpson and Seah [80] taking in account a photoelectron take-off angle of 45°.

On the other hand, the U 4f spectra recorded at surface of leached fragments (particle #2 and #3) are almost identical to pure UO_2. No Cs could be detected by XPS, see Fig. 9.

3.5. Oxidative versus non-oxidative fuel dissolution: importance for the repository

The results of the fuel leaching at room temperature at 1 bar H_2 are particularly important while discussing the redox conditions during the same type of spent fuel sample leached under flow-through conditions with the same solution under 1 bar H_2 [25]. The actual data which show very low U concentrations are in excellent agreement with NEA-TDB data on UO_2 solubility [8]. The lack of oxidized U on the fuel surface confirms the conclusion of Röllin et al. [25] that the dissolution rates measured under 1 bar H_2 with the same fuel and solution composition correspond to non-oxidative dissolution of U(IV), i.e. release of U(IV) from the solid in the under-saturated solution. In fact the presence of U(VI) in solution can be excluded for the final points from the measured total uranium concentrations corresponding to the solubility of UO_2(am) in spite of air contamination. Thus the dissolution rates measured under 1 bar hydrogen correspond to the non-oxidative dissolution of the fuel matrix. Even though these dissolution rates are 3-4 orders of magnitude lower than during leaching in presence of air, they are still high when applied to a repository. It should be kept in mind that the rate of non-oxidative dissolution of UO_2(s) is completely irrelevant for calculating fuel dissolution for repository purposes. Thus if the 0.5 g fuel used in the flow reactor in Ref. [25] would be part of the 2.7 ton fuel in a damaged copper canister placed in a repository, in order to keep the solution under-saturated and obtain the dissolution rates as measured in the reactor, flow rates of the order of 6.5 m^3/h should flow through the canister in order to correspond to the lowest flows (0.02 ml/min) used in the experimental test. This result is modified only slightly when considering details of the geometry of the reactor and of the canister: experimental reactor volume = 5 10^{-7} m^3, SA_{fuel} = 1.5 10^{-2} m^2, SA/V = 3 10^4 m^{-1}; fuel canister void volume 1 m^3, 2.7 10^6 g fuel with 0.0036 m^2/g results in SA_{fuel} = 9.72 10^3 m^2 or SA/V = 9,72 10^3 m^{-1}. Thus the SA/V value for the canister in repository is ~3 times lower than this in the experimental reactor, reducing the equivalent flow corresponding to the lowest flow in reactor to 2.2 m^3/h.

Such flows are unrealistic in a repository: the highest expected flows in a granitic repository through a deposition hole are of the order of 0.3 m^3/year [81]. From this it follows that the contribution of the non-oxidative dissolution of the fuel is negligible in the safety assessment, given that the solution in a damaged canister becomes quickly saturated with U(IV). As stated in the final report of an EU project, even with an extremely unrealistic high water flow of 1 L s^{-1} per ton of uranium (7.2 m^3/h for a canister with 2 ton U) and a specific surface area of fuel of 0.0036 m^2 g^{-1}, the solubility limit of U(IV) is achieved rapidly and U release from the fuel is solubility and not rate controlled [82].

4. Leaching of fuel fragments under 5 bar H_2-Autoclave 5U1

The same order is followed in the discussion of the results for autoclave 5U1, but this discussion is much shorter for the following

reasons. We found problems with mass 90 presence in the starting solution (originating from glass leaching or some impurity from an un-identified other source), making practically useless all ^{90}Sr ICP-MS measurements. The Viton packings of this autoclave behave somehow worse than these of 4U6, as can be judged from the increasing nitrogen levels in the gas phase from Fig. 13.

In Fig. 10, the evolution with time of the concentrations of some actinides, lanthanides and Tc in experiment 5U1 are presented. This autoclave was pressurized with 5 bar H_2 and larger fragments (originating from a different fuel pin) were leached under similar conditions as for 4U6. As can be seen, despite a washing step, there is still a pre-oxidized layer dissolved, resulting in a starting concentration of U ~10^{-6} M, almost an order of magnitude higher than in 4U6 case. The decrease of U levels is much slower than in the other test, indicating that the fuel surface area is a much more important factor for this process than the concentration of dissolved hydrogen (which is about 5 times higher here).

The decrease of the U levels is accompanied by a small but consistent decrease of the levels of Np, Tc and lanthanides. As in the case of autoclave 4U6, the most plausible explanation for the decrease of the levels of Np much lower than the solubility of NpO_2(s) is its potential co-precipitation with UO_2(s). In this test this seems to be the case also for TcO_2(s), in spite of the measurable air contamination (Fig. 13).

The lanthanides at such low concentration levels are mainly sorbed in the newly formed solid surfaces, because their concentrations increase almost to the initial levels when the temperature is raised to 70 °C and sorption probably decreases. This is not the case for Np or Tc, indicating another type of scavenging mechanism, i.e. co-precipitation with UO_2.

The evolution of the FIAP values for Cs, Mo and Sr is presented in Fig. 11. In this case a quite strong signal for mass 90 was found in the initial leaching solution in absence of fuel (shown by the horizontal dotted line in Fig. 11), which explains the erratic behaviour of Sr data during the first 100 days, where its concentrations in solution decrease. No Sr compound is expected to precipitate at such low Sr levels, thus the decrease of ^{90}(Sr+Zr) at start is probably due to sorption of ^{90}Zr from the solution to fuel and basket surfaces introduced in the autoclave at test start.

In any case, even during this test the FIAP levels of Cs and Mo are quite constant and the Fractional Release Rates FRR(t) shown in Fig. 12 are quite high at start, but after about 100 days start displaying alternate negative values even for Cs and Mo. Considering the relatively high air leakage observed during the whole duration

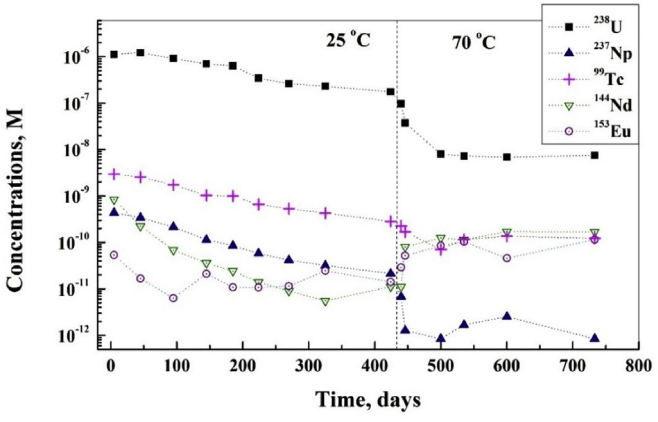

Fig. 10. Autoclave 5U1. The concentration of U, Tc, Nd, Eu and Np is plotted as a function of leaching time. Spent fuel fragments (⌀ = 2–4 mm). Starting conditions: P_{H2} = 5 bar, T = 25 °C.

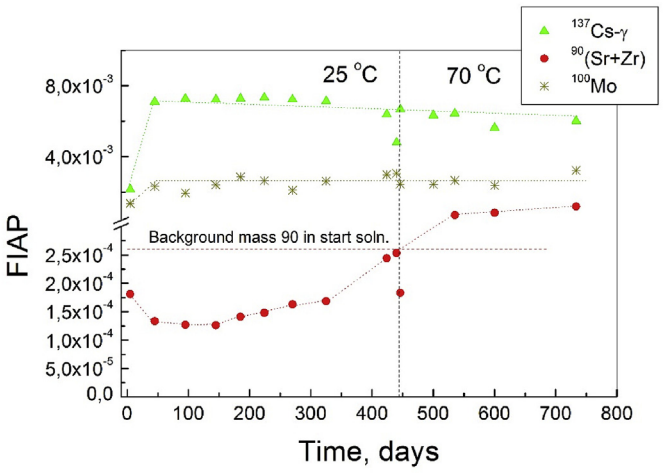

Fig. 11. Autoclave 5U1. FIAP of Cs analyzed by γ-spectroscopy, (Sr + Zr) and Mo is plotted as a function of leaching time. Spent fuel fragments (⌀ = 2–4 mm). Starting conditions: P_{H2} = 5 bar, T = 25 °C.

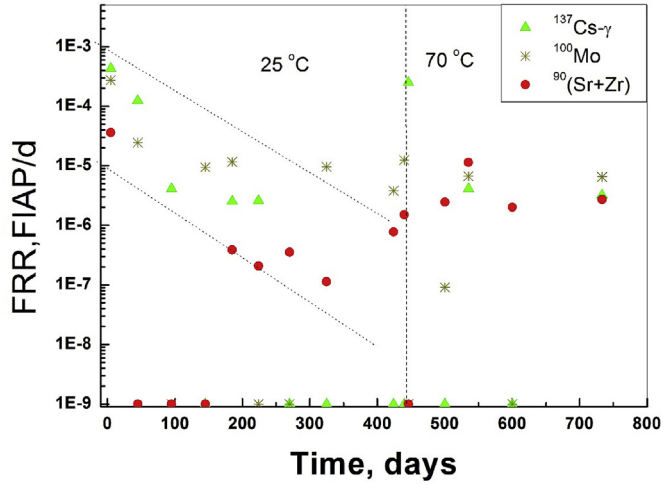

Fig. 12. Autoclave 5U1. FRR(t) (FIAP/day) for Cs measured by γ-spectrometry, Sr and Mo. Negative values of FRR for a given interval are plotted on the x-axis.

of this test as judged by the continuously increasing nitrogen levels (Fig. 13), these results indicate an extremely powerful reducing system, composed of the spent fuel surface in the presence of dissolved hydrogen. As seen from Fig-12, after ~600 days there are no more negative FRR values plotted at the x-axis, indicating that during this last period the leaching continued under oxidizing conditions, as confirmed by the measurable oxygen levels at ~730 days, see Fig. 13.

5. Uranium reduction rate

The evolution of uranium concentrations with time in the two autoclaves used in these experiments are plotted in Fig. 14 together with the extensive data for uranium reduction from Ref. [19]. As seen from Fig. 14, the reduction rate of U is substantially slower in experiment 5U2 as compared to experiment 4U6, despite the higher H_2 pressure. The main reason for this seems to be that the surface area of fuel in autoclave 4U6 is much larger than that of the fuel in autoclave 5U2 because a much finer particle size is used in 4U6 and the fuel mass is quite similar. The studies carried out by M. Jonsson's group have shown that the reaction between H_2O_2 and H_2

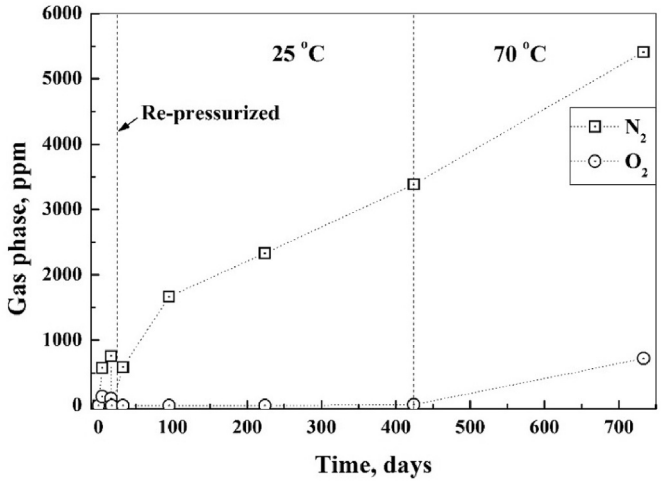

Fig. 13. Autoclave 5U1. Gas phase composition plotted as a function of leaching time. Spent fuel fragments (⌀ = 2–4 mm).

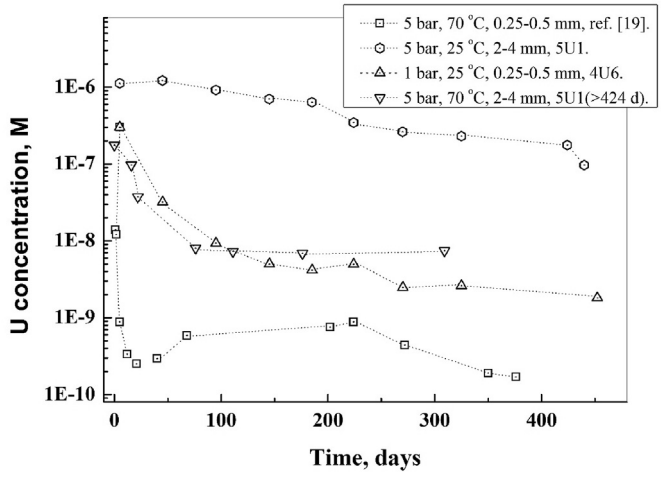

Fig. 14. Evolution of uranium concentrations in some autoclave tests.

is catalysed by Pd and is independent of the hydrogen pressure in the range 1–40 bar [83]. The reaction between H_2 and the uranyl ions UO_2^{2+} is also catalysed by Pd and is independent of the H_2 pressure in the range 1.5–40 bar [84]. Thus it seems that as long as the hydrogen concentration is above a certain limit, the consumption of the radiolytic oxidants such as H_2O_2 and the reduction of U(VI) are independent of the partial pressure of hydrogen for hydrogen pressures higher than 1 bar.

On the other hand, both fuel surface area and the temperature seem to have a large impact on the rate of reduction of U(VI) in this kind of experiments. In Table 1 the first order rate constant for the reduction of U(VI) in the initial period of the four tests plotted in Fig. 14 is reported.

The influence of temperature is seen clearly in Table 1 when comparing data for autoclave 4U6 at 25 °C with those reported in Ref. [19], where the reduction rate is about ten times faster, mainly because the temperature is 70 °C. The higher hydrogen concentration in data from ref. 19 is not expected to cause much difference, as discussed above, while the fuel surface areas are quite similar.

Table 1
First order rate constants for the reduction rate of uranyl in the various tests.

$k_{[U(VI)]}$ (h^{-1})	$m_{fuel} \approx 2$ g			
	Size = 0.25–0.5 mm		Size = 2–4 mm	
	p_{H2} = 1 bar	p_{H2} = 5 bar	p_{H2} = 5 bar	p_{H2} = 5 bar
	T = 25 °C	T = 70 °C	T = 25 °C	T = 70 °C
	1.2×10^{-3}	14×10^{-3}	0.2×10^{-3}	1.7×10^{-3}

After 424 days the temperature in autoclave 5 U1 was raised to 70 °C and the reduction rate of uranium increases and its concentration reaches levels of 6.8 10^{-9} M. As seen in Table 1, the two parts of the leaching in autoclave 5 U1 at 25 and 70 °C show clearly an increase of about eight times in the reduction rate of uranium at the higher temperature.

All this discussion can be carried only in a qualitative level because of the complexity of the system under study. Thus gas sample analysis show (Fig. 13) that there is a substantial leakage and intrusion of air in the case of autoclave 5U1. The leakage is larger than for autoclave 4U6 and could at a first sight explain also why the reduction of U is slower in this case.

Further, by comparing the initial concentrations of uranium in the two autoclaves used in these experiments, it is clearly seen that the initial U concentrations are almost one order of magnitude higher in the 5U1 autoclave, suggesting a more pre-oxidized fuel, which results in higher releases of U and fission products. This also may affect the uranium reduction rates.

6. Summary and conclusions

The experimental data presented and discussed in this paper were collected more than 10 years ago at Studsvik Nuclear, Sweden and for different reasons their publication was delayed until now. The autoclaves and the analytical instrumentation was not as good as it is today, but the tests gave answers to several questions which were important for the understanding of the hydrogen effect. Thus it was confirmed that even though Fe(II) has a known beneficial effect in counteracting the radiolytic oxidants [85], even in its absence dissolved hydrogen concentrations > 0.8 mM (corresponding to ~1 bar pressure) counteract successfully spent fuel oxidative dissolution. The choice of the fuel sample, its grain size, the solution composition and the dissolved hydrogen concentration were exactly the same as in the flow-through single pass experiments of Röllin et al. [25]. This made it possible to confirm that the concentration of hydrogen was sufficient to keep the dissolved uranium as U(IV) since under static conditions the long term uranium concentrations are in excellent agreement with the published data for the solubility of UO_2(am) [8].

We have discussed also that even though non-oxidative dissolution rates of UO_2(s) are important to measure by assuring that one works in under-saturated conditions (as done e.g. in the case of Röllin et al. [25]), they are completely irrelevant to the calculation of the fuel dissolution rates in a repository. This is because under the quasi stationary flow conditions in a damaged canister in the repository and the very low solubility of UO_2(s) under reducing conditions, the equilibrium concentration of U(IV) is reached relatively fast and then no more net U(IV) is released from the fuel matrix through this route. Only the oxidative dissolution of the UO_2(s) matrix of the spent fuel needs to be considered for performance assessment purposes.

We are not aware of any previous surface analysis of leached spent nuclear fuel by surface analytical techniques such as XPS. The extraction of the fuel grains from the autoclave under inert atmosphere was time and resource consuming, but the effort made, together with the care taken for the transportation were compensated by the results of the analysis, showing a reduced surface and the practically absent Cs from the leached surface.

In spite of the evident air contamination confirmed by gas mass analysis of the autoclave atmosphere, concordant results on the

releases of redox sensitive radionuclides and fission products such as Cs, Sr, Mo were obtained, indicating for a very strong reducing capacity of spent fuel surfaces in solutions containing more than 1 mM dissolved H_2.

We have analyzed for the first time in this work the releases of the noble metals and Mo contained in the epsilon particles of spent fuel in hydrogen saturated solutions and found them practically constant during the more than two yearlong tests, with no indication of any measurable release rate.

Finally, the decrease of the concentrations of uranium and other redox sensitive radionuclides under our test conditions depends strongly on the fuel surface area and temperature, while the hydrogen pressure has not any marked effect, provided it is over a threshold limit.

Declaration of competing interest

The authors declare that they have no known competing financial interests or personal relationships that could have appeared to influence the work reported in this paper.

Acknowledgements

The authors would like to thank J. Low, V. Flygare and B. Sundström for help with hot cell work as well as R-M. Carlsson and R.Gejland for help with radiation protection work at Studsvik Nuclear AB. This work was supported by Swedish Nuclear Fuel and Waste Management Co. (SKB).

References

[1] H. Kleykamp, The chemical state of the fission products in oxide fuels, J. Nucl. Mater. 131 (1985) 221–246.
[2] L.H. Johnson, D.W. Shoesmith, Spent fuel, in: W. Lutze, R.C. Ewing (Eds.), Radioactive Waste Forms for the Future, North-Holland Physics Publishing, The Netherlands, 1988.
[3] S. Imoto, Chemical state of fission products in irradiated UO_2, J. Nucl. Mater. 140 (1986) 19–27.
[4] H. Kleykamp, The solubility of selected fission products in UO_2 and (U, Pu)O_2, J. Nucl. Mater. 206 (1993) 82–86.
[5] D.W. Shoesmith, Fuel corrosion processes under waste disposal conditions, J. Nucl. Mater. 282 (2000) 1–31.
[6] P. Wersin, K. Spahiu, J. Bruno, Time Evolution of Oxygen and Redox Conditions in HLW Repository, SKB TR 94-02, Stockholm, 1994.
[7] I. Puigdomenech, L. Trotignon, S. Kotelnikova, K. Pedersen, L. Griffault, V. Michaud, J.-E. Lartigue, K. Hama, H. Yoshida, J. West, K. Bateman, A. Milodowski, S. Banwart, J. Rivas Perez, E.-L. Tullborg, O_2 consumption in a granitic environment, Mater. Res. Soc. Symp. Proc. 608 (2000) 179–184.
[8] G. Guillamont, et al., Chemical Thermodynamics, vol. 5, Elsevier, Amsterdam, 2003.
[9] J.W.T. Spinks, R.J. Wood, An Introduction on Radiation Chemistry, third ed., John Wiley & Sons Inc., New York, 1990.
[10] NAGRA Technical Report NTB 04-09, Wettingen Switzerland, in: L.H. Johnson (Ed.), Spent Fuel Evolution under Disposal Conditions, vol. 2005, 2005.
[11] B. Bonin, A. Colin, A. Dutfoy, Pressure building during early stages of gas production in a radioactive waste repository, J. Nucl. Mater. 281 (2000) 1–14.
[12] R.M. Garrels, C.L. Christ, Solutions, Minerals, and Equilibria, Harper & Row, New York, 1965.
[13] L. Liu, I. Neretnieks, The effect of hydrogen on oxidative dissolution of spent fuel, Nucl. Technol. 138 (2002) 69–77.
[14] P. Sellin, SR 97: hydromechanical evolution in a defective canister, Mater. Res. Soc. Symp. Proc. 663 (2002) 755–763.
[15] K. Spahiu, L. Werme, U.-B. Eklund, The influence of near field hydrogen on actinide solubilities and spent fuel leaching, Radiochim. Acta 88 (2000) 507–511.
[16] K. Spahiu, U.-B. Eklund, D. Cui, M. Lundström, The influence of near field redox conditions on spent fuel leaching, Mater. Res. Soc. Symp. Proc. 713 (2002) 633–638.
[17] A. Loida, B. Grambow, H. Geckeis, Spent fuel corrosion behavior in salt solution in the presence of hydrogen overpressure, in: Proc. ICEM'01, 8th Internat. Conf. On Radioactive Waste Management, 2001. Bruges, Belgium.
[18] A. Loida, V. Metz, B. Kienzler, H. Geckeis, Radionuclide release from high burnup spent fuel during corrosion in salt brine in the presence of hydrogen overpressure, J. Nucl. Mater. 346 (2005) 24–31.
[19] K. Spahiu, D. Cui, M. Lundström, The fate of radiolytic oxidants during spent fuel leaching in the presence of dissolved near field hydrogen, Radiochim. Acta 92 (2004) 625–629.
[20] P. Fors, P. Cabol, S. Van Winkel, K. Spahiu, Corrosion of high burn-up structured UO_2 fuel in the presence of dissolved H_2, J. Nucl. Mater. 394 (2009) 1–8.
[21] P. Carbol, P. Fors, S. Van Winckel, K. Spahiu, Corrosion of irradiated MOX fuel in presence of dissolved H_2, J. Nucl. Mater. 392 (2009) 45–54.
[22] A. Puranen, A. Barreiro, L.Z. Evins, K. Spahiu, Spent fuel leaching in the presence of corroding iron, MRS Adv. Energy Sustain. 1 (12) (2016) 681–686.
[23] B. Grambow, A. Loida, A. Martinez-Esparza, P. Diaz-Arocas, J. de Pablo, J.-L. Paul, G. Marx, J.-P. Glatz, K. Lemmens, K. Ollila, H. Christensen, Source Term for Performance Assessment of Spent Fuel as a Waste Form, EUR 19140 EN, 2000.
[24] A. Loida, B. Grambow, H. Geckeis, Anoxic corrosion of various high burnup spent fuel samples, J. Nucl. Mater. 238 (1996) 11–22.
[25] S. Röllin, K. Spahiu, U.-B. Eklund, Determination of dissolution rates of spent fuel in carbonate solutions under different redox conditions with a flow-through experiment, J. Nucl. Mater. 297 (2001) 231–243.
[26] L. Werme, L. Johnson, V. Oversby, B. Grambow, F. King, K. Spahiu, D.W. Shoesmith, Spent Fuel Performance under Repository Conditions: A Model for Use in SR-Can, SKB TR-04-19, Stockholm, 2004.
[27] G.A. Parks, D.C. Pohl, Hydrothermal solubility of uraninite, Geochem. Cosmochim. Acta 52 (1988) 863–875.
[28] R. Forsyth, reportFuel Rod D07-B15 from Ringhals 2 PWR: Source Material for Corrosion/leach Tests in Groundwater. Fuel Pellet Characterization Program, Part I, SKB Technical Report 87-02, Stockholm1987.
[29] U.-B. Eklund, R. Forsyth, Fuel Rod 03688 from Ringhals 2: Measurement of Fission Gas Release and Burnup, Studsvik Technical Note NF, 1987 (P)-87-16.
[30] R. Forsyth, Reference BWR Fuel Corrosion Tests (Oskarshamn 1 Rod O1-418-A6), SKB Arbetsrapport 94-06, Stockholm, 1994.
[31] B. Grambow, A. Loida, P. Dressler, H. Geckeis, J. Gago, I. Casas, J. de Pablo, J. Gimenez, M.E. Torrero, Long-term Safety of Radioactive Waste Disposal: Chemical Reaction of Fabricated and High Burnup Spent Fuel with Saline Brines, FZK Report FZKA 5702, 1996. Karlsruhe.
[32] C. Jegou, S. Peuget, V. Broudic, D. Roudil, V. Deschanels, J.M. Bart, Identification of the mechanism limiting the alteration of clad spent fuel segments in aerated carbonated groundwater, J. Nucl. Mater. 326 (2004) 144–155.
[33] M.P. Seah, I.S. Gilmore, G. Beamson, XPS: binding energy calibration of electron spectrometers 5 – Re-evaluation of the reference energies, Surf. Interface Anal. 26 (1998) 642–649.
[34] I. Perez, I. Casas, M. Martin, J. Bruno, Thermodynamics and kinetics of uranophane dissolution in bicarbonate test solutions, Geochem. Cosmochim. Acta 64 (2000) 603–608.
[35] B. Hanson, B. McNamara, E. Buck, J. Friese, E. Jensen, K. Krupka, B. Arey, Corrosion of commercial spent nuclear fuel, 1. Formation of studtite and metastudtite, Radiochim. Acta 95 (2005) 159–168.
[36] B. McNamara, B. Hansen, E. Buck, C. Soderquist, Corrosion of commercial spent nuclear fuel, 2. Radiochemical analyses of metastudtite and leachates, Radiochim. Acta 93 (2005) 169–175.
[37] C. Jegou, B. Muzeau, V. Brudic, S. Peuget, A. Poulesquen, D. Rudil, C. Corbel, Effect of external gamma radiation on dissolution of the spent UO_2 fuel matrix, J. Nucl. Mater. 341 (2005) 62–82.
[38] G. Sattonay, C. Ardois, C. Corbel, J.F. Lucchini, M.-F. Barthe, F. Garrido, D. Gosset, Alpha-radiolysis effects on UO_2 alteration in water, J. Nucl. Mater. 288 (2001) 11–19.
[39] K.-A. Hughes Kubatko, K.B. Helean, A. Navrotsky, P.C. Burns, Stability of peroxide-containing uranyl minerals, Science 302 (2003) 1191–1193.
[40] M. Amme, Contrary effects of the water radiolysis product H_2O_2 upon the dissolution of nuclear fuel in natural ground waters and deionised water, Radiochim. Acta 90 (2002) 399–406.
[41] H. Christensen, Radiation induced dissolution of UO_2, MRS Symp. Proc. 212 (1991) 213–218.
[42] F.B. Baker, T.W. Newton, The reaction between U(IV) and hydrogen peroxide, J. Phys. Chem. 65 (1961) 1897–1899.
[43] A.J. Elliot, S. Padamshi, J. Pika, Free radical redox reactions of uranium ions in sulphuric acid solutions, Can. J. Chem. 64 (1986) 314–320.
[44] K.H. Schmidt, Measurement of the activation energy for the reaction of the hydroxyl radical with hydrogen in aqueous solution, J. Phys. Chem. 81 (1977) 1257–1263.
[45] H. Christensen, K. Sehested, Reaction of hydroxyl radicals with hydrogen at elevated temperatures. Determination of the activation energy, J. Phys. Chem. 87 (1983) 118–120.
[46] M. Jonsson, F. Nielsen, E. Ekeroth, T. Eriksen, Modeling effects of radiolysis on UO_2-dissolution employing recent experimental data, MRS Symp. Proc. 807 (2004) 385–390.
[47] S. Nilsson, M. Jonsson, H_2O_2 and radiation induced dissolution of UO_2 and SIMFUEL pellets, J. Nucl. Mater. 410 (2011) 89–93.
[48] L. Bauhn, N. Hansson, C. Ekberg, P. Fors, K. Spahiu, The fate of hydroxyl radicals produced during the decomposition of H_2O_2 on a SIMFUEL surface in the presence of dissolved hydrogen, J. Nucl. Mater. 222 (2018) 33–46.
[49] P. Carbol, J. Cobos-Sabate, J.-P. Glatz, B. Grambow, B. Kienzler, A. Loida, A. Martinez Esparza, V. Metz, J. Quiñones, C. Ronchi, V. Rondinella, K. Spahiu, D. Wegen, T. Wiss, The Effect of Dissolved Hydrogen on the Dissolution of ^{233}U Doped UO_2(s), High Burnup Spent Fuel and MOX Fuel, SKB Technical Report TR 05-09, 2005.
[50] D. Rai, A.R. Felmy, J.L. Ryan, Uranium(IV) hydrolysis constants and the

solubility of $UO_2.xH_2O$(am), Inorg. Chem. 29 (1990) 260–264.
[51] T.W. Newton, ERDA Critical Review Series, NTIS, Springfield VA, 1975.
[52] J. Halpern, J.G. Smith, Kinetics of the oxidation of uranium (IV) by molecular oxygen in aqueous perchloric acid solutions, Can. J. Chem. 34 (1956) 1419–1427.
[53] D. Cui, E. Ekeroth, P. Fors, K. Spahiu, Surface mediated processes in the interaction of spent fuel or α-doped UO_2 with H_2, MRS Symp. Proc. V. 1104 (2008) 87–99.
[54] T. Eriksen, P. Ndalamba, D. Cui, J. Bruno, M. Caceci, K. Spahiu, Solubility of the redox sensitive radionuclides ^{99}Tc and ^{237} Np under reducing conditions in neutral to alkaline solutions. Effect of carbonate, SKB Technical Report TR 93-18, 1993.
[55] D. Rai, N. Hess, M. Yui, A. Felmy, D. Moore, Thermodynamics and solubility of $U_xNp_{1-x}O_2$ (am) solid solutions in the carbonate system, Radiochim. Acta 92 (2004) 527–535.
[56] H-U. Zwicky, J. Low, E. Ekeroth, reportCorrosion Studies with High Burnup Light Water Reactor Fuel, SKB Technical Report TR-11-03, Stockholm 2011.
[57] J.-P. Crocombette, Ab initio energetics of some fission products (Kr, I, Cs, Sr and He) in uranium dioxide, J. Nucl. Mater. 305 (2002) 29–36.
[58] K. Spahiu, U.-B. Eklund, D. Cui, M. Lundström, The influence of near field redox conditions on spent fuel leaching, Mater. Res. Soc. Symp. 713 (2002) 633–638.
[59] A. Loida, R. Gens, C. Bube, K. Lemmens, C. Cachoir, T. Mennecart, B. Kienzler, Corrosion behavior of spent fuel in high pH solutions-Effect of hydrogen, MRS Symp. Proc. 1475 (2012) 119–124.
[60] P.L. Brown, C. Ekberg, Hydrolysis of Metal Ions, vol. 2, Wiley-VCH, Verlag GmbH&Co. KGaA, Boschstr, 2016, 12, 69469 Weinheim, Germany 2016.
[61] W. Hummel, Chemistry of Selected Dose Relevant Nuclides, NAGRA Technical Report NTB 17-05, March 2017. Wettingen, Switzerland.
[62] V.K. Kozlov, I.L. Khodakovskiy, The thermodynamic parameters of atomic silver in aqueous solution at 25-280 °C (translated from Geokhimiya 6 (1983) 836-848), Geochem. Int. 20 (1983) 118–131.
[63] J. Dobrowolski, J. Oglaza, Zastoswanie izotopu ^{110}Ag do badania rozpuszczalnosci srebra metalicznego i chlorku srebra w roztworach wodnych siarczanu cynku [Use of the isotope ^{110}Ag to study the solubility of silver metal and silver chloride in aqueous solutions of zinc sulphide], Nucleonika 8 (1963) 79–81 (in Polish).
[64] D. Cui, T. Eriksen, U.-B. Eklund, On metal aggregates in spent fuel, synthesis and leaching of Mo-Ru-Pd-Rh alloy, MRS Symp. Proc. 663 (2001) 427–434.
[65] D. Cui, J. Low, C.J. Sjöstedt, K. Spahiu, On Mo-Ru-Tc-Pd-Rh alloy particles extracted from spent fuel and their leaching behaviour under anoxic conditions, Radiochim. Acta 92 (2004) 551–555.
[66] Y. Albinsson, A. Jensen, V. Oversby, L. Werme, Leaching of spent fuel under anaerobic and reducing conditions, MRS Symp. Proc. 757 (2003) 407–413.
[67] S. Utsunomiya, R.C. Ewing, Thee fate of epsilon phase (Mo-Ru-Pd-Tc-Rh) in the UO_2 of the Oklo natural fission reactors, Radiochim. Acta 94 (2006) 749–753.
[68] V. Metz, H. Geckeis, E. Gonzáles-Robles, A. Loida, C. Bube, B. Kienzler, Radionuclide behaviour in the near-field of a geological repository for spent nuclear fuel, Radiochim. Acta 100 (2012) 699–713.
[69] E.S. Ilton, P.S. Bagus, XPS determination of uranium oxidation states, Surf. Interface Anal. 43 (2011) 1549–1560.
[70] NIST, X-ray Photoelectron Spectroscopy Database, Version 4.1, National Institute of Standards and Technology, Gaithesburg, 2012. http://srdata.nist.gov/xps/.
[71] B.G. Santos, H.W. Nesbitt, J.J. Noel, D.W. Shoesmith, X-ray photoelectron spectroscopy study of anodically oxidized SIMFUEL surfaces, Electrochim. Acta 49 (2004) 1863–1873.
[72] M. Razdan, D.W. Shoesmith, Influence of trivalent dopants on the structural and electrochemical properties of UO_2, J. Electrochem. Soc. 161 (2014) H105–H113.
[73] D. Prieur, L. Martel, J.-F. Vigier, A.C. Scheinost, K.O. Kvashnina, J. Sommers, P.M. Martin, Aliovalent cation substitution in UO_2 : electronic and local structures of $U_{1-y}La_yO_{2+x}$ solid solutions, Inorg. Chem. 57 (2018) 1535–1544.
[74] D. Prieur, P.M. Martin, A. Jankowiak, E. Gavilan, A.C. Scheinost, N. Herlet, P. Dehaudt, P. Blanchart, Local structure and charge distribution in mixed uranium-americium oxides : effect of oxygen potential and Am content, Inorg. Chem. 50 (2011) 12437–12445.
[75] D. Prieur, P.M. Martin, F. Lebreton, T. Delahaye, D. Banerjee, A. Scheinost, A. Jankowiak, Accommodation of multivalent cations in fluorite type solid solutions : case of Am-bearing UO_2, J. Nucl. Mater. 434 (2013) 7–16.
[76] S.M. Butorin, K.O. Kvashnina, D. Prieur, M. Rivenet, P.M. Martin, Characteristics of chemical bonding of pentavalent uranium in La-doped UO_2, Chem. Commun. 53 (2017) 115–118.
[77] J. de Pablo, I. Casas, J. Gimenez, V. Marti, M.E. Torrero, Solid surface evolution model to predict uranium release from unirradiated UO_2 and nuclear spent fuel dissolution under oxidizing conditions, J. Nucl. Mater. 232 (1996) 138–145.
[78] J. de Pablo, I. Casas, J. Gimenez, M. Molera, M. Rovira, L. Duro, J. Bruno, The oxidative dissolution mechanism of uranium dioxide. I. The effect of temperature in hydrogen carbonate medium, Geochem. Cosmochim. Acta 63 (1999) 3097–3103.
[79] P. Carbol, P. Fors, T. Gouder, K. Spahiu, Hydrogen suppresses nuclear waste corrosion, Geochem. Cosmochim. Acta 73 (2009) 4366–4375.
[80] P.J. Cumpson, M.P. Seah, Elastic scattering corrections in AES and XPS. II. Estimating attenuation lengths and conditions required for their valid use in overlayer/substrate experiments, Surf. Interface Anal. 25 (1997) 430–446.
[81] SKB, Long-term safety for the final repository for spent nuclear fuel at Forsmark, Main report for the SR-Site project, SKB-TR-11-01, Stockholm, 2011.
[82] B. Grambow, J. Bruno, L. Duro, J. Merino, A. Tamayo, C. Martin, G. Pepin, S. Schumacher, O. Smidt, C. Ferry, C. Jegou, J. Quinones, E. Iglesias, N. Rodrigues Villagra, J.M. Nieto, A. Martinez-Esparza, A. Loida, V. Metz, B. Kienzler, G. Bracke, D. Pellegrini, G. Mathieu, V. Wasselin-Trupin, C. Serres, D. Wegen, M. Jonsson, L. Johnson, K. Lemmens, J. Liu, K. Spahiu, E. Ekeroth, I. Casas, J. de Pablo, C. Watsson, P. Robinson, D. Hodgkinson, Final Activity Report: EU-Project MICADO (Model Uncertainty for the Mechanism of Dissolution of Spent Nuclear Fuel in a Waste Repository), March 2010, 60 p.
[83] S. Nilsson, M. Jonsson, On the catalytic effects of UO_2(s) and Pd(s) on the reaction between H_2O_2 and H_2 in aqueous solutions, J. Nucl. Mater. 372 (2008) 160–163.
[84] S. Nilsson, M. Jonsson, On the catalytic effects of Pd(s) on the reduction of UO_2^{2+} with H_2 in aqueous solutions, J. Nucl. Mater. 374 (2008) 290–292.
[85] M. Jonsson, F. Nielsen, O. Roth, E. Ekeroth, S. Nilsson, M.M. Hossain, Radiation induced spent nuclear fuel dissolution under deep repository conditions, Environ. Sci. Technol. 41 (2007) 7087–7093.